



**HAL**  
open science

# Circle criterion-based $\mathcal{H}_\infty$ observer design for Lipschitz and monotonic nonlinear systems - Enhanced LMI conditions and constructive discussions

Ali Zemouche, Rajesh Rajamani, Gridsada Phanomchoeng, Boulaïd Boulkroune, Hugues Rafaralahy, Michel Zasadzinski

## ► To cite this version:

Ali Zemouche, Rajesh Rajamani, Gridsada Phanomchoeng, Boulaïd Boulkroune, Hugues Rafaralahy, et al.. Circle criterion-based  $\mathcal{H}_\infty$  observer design for Lipschitz and monotonic nonlinear systems - Enhanced LMI conditions and constructive discussions. *Automatica*, 2017, 85, pp.412-425. 10.1016/j.automatica.2017.07.067 . hal-01567360

**HAL Id: hal-01567360**

**<https://hal.science/hal-01567360>**

Submitted on 12 Jan 2018

**HAL** is a multi-disciplinary open access archive for the deposit and dissemination of scientific research documents, whether they are published or not. The documents may come from teaching and research institutions in France or abroad, or from public or private research centers.

L'archive ouverte pluridisciplinaire **HAL**, est destinée au dépôt et à la diffusion de documents scientifiques de niveau recherche, publiés ou non, émanant des établissements d'enseignement et de recherche français ou étrangers, des laboratoires publics ou privés.

# Circle Criterion-Based $\mathcal{H}_\infty$ Observer Design for Lipschitz and Monotonic Nonlinear Systems - Enhanced LMI Conditions and Constructive Discussions

A. Zemouche <sup>a,b</sup>, R. Rajamani <sup>c</sup>, G. Phanomchoeng <sup>d</sup>, B. Boukroune <sup>e</sup>, H. Rafaralahy <sup>a</sup>,  
M. Zasadzinski <sup>a</sup>

<sup>a</sup>University of Lorraine, CRAN UMR CNRS 7039, 54400 Cosnes et Romain, France.

<sup>b</sup>EPI Inria DISCO, Laboratoire des Signaux et Systèmes, CNRS-CentraleSupélec, 91192 Gif-sur-Yvette, France.

<sup>c</sup>Laboratory for Innovations in Sensing, Estimation, and Control, Department of Mechanical Engineering, University of Minnesota, Minneapolis, USA.

<sup>d</sup>Department of Mechanical Engineering, Faculty of Engineering, Chulalongkorn University, Bangkok 10330, Thailand.

<sup>e</sup>Einderpad, 20A, 3920 Lommel, Belgium.

---

## Abstract

A new LMI design technique is developed to address the problem of circle criterion-based  $\mathcal{H}_\infty$  observer design for nonlinear systems. The developed technique applies to both locally Lipschitz as well as monotonic nonlinear systems, and allows for nonlinear functions in both the process dynamics and output equations. The LMI design condition obtained is less conservative than all previous results proposed in literature for these classes of nonlinear systems. By judicious use of a modified Young's relation, additional degrees of freedom are included in the observer design. These additional decision variables enable improvements in the feasibility of the obtained LMI. Several recent results in literature are shown to be particular cases of the more general observer design methodology developed in this paper. Illustrative examples are given to show the effectiveness of the proposed methodology. The application of the method to slip angle estimation in automotive applications is discussed and experimental results are presented.

*Key words:* Observers design; Lipschitz systems; LMI approach;  $\mathcal{H}_\infty$  synthesis; slip angle estimation.

---

## 1 Introduction and Preliminaries

### 1.1 Introduction

Observer design for nonlinear systems has attracted much research interest in recent years. This is due to the important role of observers for the estimation of unmeasurable variables, that are increasingly present in modern real-world applications, such as intelligent vehicles (Rajamani, 2012), electrical machines (Khalil, 2015), position estimation in

industrial systems (Henriksson *et al.*, 2009), and biomedical applications (Chong *et al.*, 2012). The emergence of automation in many real world applications renders the estimation problem very important. In addition to the estimation of unmeasurable variables, observers play critical roles in the fields of fault diagnosis, feedback control and automated event detection.

Although state observer design has been widely investigated in the literature and numerous methods have been established (Thau, 1973), (Krener and Respondek, 1985), (Gauthier *et al.*, 1992), (Gauthier and Kupka, 1994), (Arcak and Kokotovic, 2001), (Khalil, 2002), (Fan and Arcak, 2003), (Califano *et al.*, 2003), (Kravaris *et al.*, 2004), (Simon, n.d.), (Kravaris *et al.*, 2007), this issue remains a challenge for the control research community. Several new methods have been developed in the recent literature (Ibrir, 2007), (Tsinias,

---

*Email address:* ali.zemouche@univ-lorraine.fr (A. Zemouche).

<sup>1</sup> A portion of the work in this paper was funded by the US National Science Foundation GRANT CMMI 1562006. The second portion of the work was supported by the Inria–Saclay, EPI DISCO.

2008), (Abbaszadeh and Marquez, 2010), (Phanomchoeng *et al.*, 2011), (Zemouche and Boutayeb, 2013), (Açikmese and Corless, 2011), (Alessandri and Rossi, 2013), (Alessandri and Rossi, 2015), (Andrieu *et al.*, 2009), (Astolfi and Marconi, 2015), (Astolfi *et al.*, 2016), (Wang *et al.*, 2017). All these techniques have been motivated by the lack of a general systematic method to deal with nonlinear systems. Even if many improvements have been proposed in the recent years (Oueder *et al.*, 2012), (Zemouche and Boutayeb, 2013), (Açikmese and Corless, 2011), the estimation problem still remains open. Particularly, for the class of globally Lipschitz nonlinear systems, several LMI methods have been proposed where each method provides a new LMI technique. For instance, some techniques are based on the use of the S-Procedure lemma (Boyd *et al.*, 1994); others use Riccati equations (Raghavan and Hedrick, 1994), and finally some are based on the standard use of Young's inequality (Alessandri, 2004). A two degree-of-freedom observer design method has been proposed in Arcak and Kokotovic (2001), generalized by Zemouche and Boutayeb (2009). Despite all these new ways to overcome the effect of the nonlinearities, the proposed methods remain conservative for some classes of systems. To improve the existing results, an interesting method was proposed recently in Chong *et al.* (2012) by introducing a diagonal multiplier matrix as an additional degree of freedom. Such a technique has been shortly discussed in Fan and Arcak (2003) for a class of systems with monotonic nonlinearities. Although the introduction of a diagonal multiplier matrix is interesting and significant, some improvements remain possible. The main question that arises naturally is: why not a non diagonal multiplier matrix? The answer to this question is one of the main subjects of this paper. A short and preliminary version of this result has been presented in Zemouche *et al.* (2016) as a conference paper. Indeed, a new relaxed LMI condition is provided to solve the problem of  $\mathcal{H}_\infty$  observer synthesis by exploiting the Young's relation in a judicious manner. This novel way to use the Young's inequality allows to have additional degrees of freedom in the LMI and to avoid the diagonal form of the multiplier matrix. Further, the developed results are extended to nonlinear systems that are monotonic and not necessarily globally Lipschitz, and further to systems that contain nonlinearities in the output equation. To clarify the presentation of this paper, let us note that compared to the preliminary conference version paper (Zemouche *et al.*, 2016), this extended version contains:

- Nonlinearities in the output equation while the conference paper had only a linear measurement equation;
- vehicle slip angle estimation which is a real-world application and further includes experimental results;
- additional example to show the role of the non diagonal multiplier matrices;
- extended discussions and some analytic comparisons.

The developed  $\mathcal{H}_\infty$  observer can be applied for many practical problems. The vehicle slip angle estimation is one of the challenging problems which can be solved by the method. The feedback of vehicle slip angle is useful for

Electronic Stability Control (ESC) systems. In situations on low-friction road surfaces, it is useful for the ESC system to control the vehicle slip angle and prevent the vehicle slip angle from being too high (Phanomchoeng *et al.*, 2011). However, vehicle slip angle cannot easily measured. The vehicle slip angle is also not easy to estimate due to the nonlinear tire model. Both the dynamic and measurement models of the system are highly nonlinear models (Phanomchoeng *et al.*, 2011).

In this paper, the proposed  $\mathcal{H}_\infty$  observer was used to estimate the vehicle slip angle based on a nonlinear vehicle model. The observer is shown to be suitable for a large range of operating conditions. The developed technique is validated with experimental measurements on a test vehicle, under different road conditions.

The rest of the paper is organized as follows: after some useful preliminaries, the problem formulation and the preliminary result of Zemouche *et al.* (2016) are introduced in Section 2, in order to well position what we propose. The main contribution related to the new LMI observer design method extended to systems with nonlinear outputs is presented in Section 3. Section 4 presents discussions and comparisons with previous results in literature. Two simple but relevant examples are proposed in Section 5 to show the efficiency of the proposed design methodology. Section 6 includes the design of an observer and experimental results for the application of slip angle estimation in automobiles. Finally, we end the paper by a conclusion in Section 7.

**Notations:** Throughout this paper, we use the following notations:

- $(\star)$  is used for the blocks induced by symmetry;
- $A^T$  represents the transposed matrix of  $A$ ;
- $\mathbb{I}_r$  represents the identity matrix of dimension  $r$ ;
- for a square matrix  $S$ ,  $S > 0$  ( $S < 0$ ) means that this matrix is positive definite (negative definite);
- $e_s(i) = \underbrace{(0, \dots, 0, \overset{i \text{ th}}{1}, 0, \dots, 0)}_{s \text{ components}}^T \in \mathbb{R}^s, s \geq 1$  is a vector of the canonical basis of  $\mathbb{R}^s$ .

## 1.2 Some preliminaries

We start by introducing some definitions and preliminaries which will be used throughout this paper.

**Definition 1 (Zemouche and Boutayeb (2013))** Consider two vectors

$$X = \begin{pmatrix} x_1 \\ \vdots \\ x_n \end{pmatrix} \in \mathbb{R}^n \text{ and } Y = \begin{pmatrix} y_1 \\ \vdots \\ y_n \end{pmatrix} \in \mathbb{R}^n.$$

For all  $i = 0, \dots, n$ , we define an auxiliary vector  $X^{Y_i} \in \mathbb{R}^n$  corresponding to  $X$  and  $Y$  as follows:

$$\left\{ \begin{array}{l} X^{Y_i} = \begin{pmatrix} y_1 \\ \vdots \\ y_i \\ x_{i+1} \\ \vdots \\ x_n \end{pmatrix} \text{ for } i = 1, \dots, n \\ X^{Y_0} = X \end{array} \right. \quad (1)$$

**Lemma 2 (Zemouche and Boutayeb (2013))** Consider a function  $\Psi : \mathbb{R}^n \rightarrow \mathbb{R}^n$ . Then, the two following items are equivalent:

- $\Psi$  is globally Lipschitz with respect to its argument, i.e.:

$$\|\Psi(X) - \Psi(Y)\| \leq \gamma_{\Psi} \|X - Y\|, \quad \forall X, Y \in \mathbb{R}^n \quad (2)$$

- for all  $i, j = 1, \dots, n$ , there exist functions

$$\psi_{ij} : \mathbb{R}^n \times \mathbb{R}^n \rightarrow \mathbb{R}$$

and constants  $\underline{\gamma}_{\psi_{ij}}$  and  $\bar{\gamma}_{\psi_{ij}}$  such that  $\forall X, Y \in \mathbb{R}^n$

$$\Psi(X) - \Psi(Y) = \sum_{i=1}^n \sum_{j=1}^n \psi_{ij} \mathcal{H}_{ij}(X - Y) \quad (3)$$

and the functions  $\psi_{ij}(\cdot)$  are globally bounded from above and below as follows:

$$\underline{\gamma}_{\psi_{ij}} \leq \psi_{ij} \leq \bar{\gamma}_{\psi_{ij}} \quad (4)$$

where

$$\psi_{ij} \triangleq \psi_{ij}(X^{Y_{j-1}}, X^{Y_j}) \text{ and } \mathcal{H}_{ij} = e_n(i) e_n^T(j)$$

**PROOF.** The proof is omitted. See Zemouche and Boutayeb (2013).

The following lemma is very useful for the proposed new LMI design.

**Lemma 3 (Zemouche et al. (2016))** Let  $X$  and  $Y$  be two given matrices of appropriate dimensions. Then, for any

symmetric positive definite matrix  $S$  of appropriate dimension, the following inequality holds:

$$X^T Y + Y^T X \leq \frac{1}{2} [X + SY]^T S^{-1} [X + SY]. \quad (5)$$

The significance of Lemma 3 does not lie in its proof that is trivial, but its main strength to retain is that only the half quantity of  $X^T Y + Y^T X$  is upper bounded by the Young's relation. It is worth to notice that it is the first time the Young's inequality is used under this form. It plays an important role because it leads to less conservative LMI synthesis conditions.

## 2 Problem Formulation and Preliminary Result

### 2.1 Problem formulation

For simplicity of the presentation, we start by investigating nonlinear systems depending only on the system state and with linear outputs. The system is described by the following equations:

$$\begin{cases} \dot{x} = Ax + G\gamma(x) + E\omega \\ y = Cx + D\omega \end{cases} \quad (6)$$

where  $x \in \mathbb{R}^n$  is the state vector,  $y \in \mathbb{R}^p$  is the output measurement,  $\omega \in \mathbb{R}^q$  is the disturbance  $\mathcal{L}_2$  bounded vector. The matrices  $A \in \mathbb{R}^{n \times n}$ ,  $G \in \mathbb{R}^{n \times m}$ ,  $E \in \mathbb{R}^{n \times q}$ ,  $C \in \mathbb{R}^{p \times n}$ ,  $D \in \mathbb{R}^{p \times q}$  are constant. To begin with the nonlinear function  $\gamma : \mathbb{R}^n \rightarrow \mathbb{R}^m$  is assumed to be globally Lipschitz. Notice that the fact we use the same disturbances vector  $\omega$  in the dynamics and the output measurements is not a restriction because the matrices  $E$ ,  $D$  and the dimension of  $\omega$  are arbitrary. Indeed, if we assume that in the dynamics we have  $E_1 \omega_1$ , and in the measurement equation, we have  $E_2 \omega_2$ , then

we can always write  $E = [E_1 \ 0]$ ,  $D = [0 \ E_2]$  and  $\omega = \begin{bmatrix} \omega_1 \\ \omega_2 \end{bmatrix}$ ,

which lead to the form (6). Before introducing the observer, let us consider  $\gamma(\cdot)$  under the detailed form:

$$\gamma(x) = \begin{bmatrix} \gamma_1(H_1 x) \\ \vdots \\ \underbrace{\vartheta_i}_{\gamma_i(H_i x)} \\ \vdots \\ \gamma_m(H_m x) \end{bmatrix} \quad (7)$$

where  $H_i \in \mathbb{R}^{n_i \times n}$ . Notice that the  $n_i$ , which represents the number of rows of  $H_i$  are not constrained. The matrices  $H_i$  are not unique and then  $n_i$  are free. This is, indeed, an advantage of the proposed approach compared to those using

diagonal multiplier matrices (Fan and Arcak, 2003), (Chong *et al.*, 2012).

We use the following generalized Arcak's observer form:

$$\dot{\hat{x}} = A\hat{x} + G \begin{bmatrix} \gamma_1(\hat{\vartheta}_1) \\ \vdots \\ \gamma_i(\hat{\vartheta}_i) \\ \vdots \\ \gamma_m(\hat{\vartheta}_m) \end{bmatrix} + L(y - C\hat{x}) \quad (8a)$$

$$\dot{\hat{\vartheta}}_i = H_i\hat{x} + K_i(y - C\hat{x}) \quad (8b)$$

where  $\hat{x}$  is the estimate of  $x$ . the matrices  $L \in \mathbb{R}^{n \times p}$  and  $K_i \in \mathbb{R}^{n_i \times p}$  are the observer parameters to be determined so that the estimation error  $e = x - \hat{x}$  converges asymptotically towards zero.

Since  $\gamma(\cdot)$  is globally Lipschitz, then from Lemma 2 there exist functions

$$\phi_{ij} : \mathbb{R}^{n_i} \times \mathbb{R}^{n_i} \longrightarrow \mathbb{R}$$

and constants  $a_{ij}, b_{ij}$ , such that

$$\gamma(x) - \gamma(\hat{x}) = \sum_{i,j=1}^{i,j=m,n_i} \phi_{ij} \mathcal{H}_{ij} (\vartheta_i - \hat{\vartheta}_i) \quad (9)$$

and

$$a_{ij} \leq \phi_{ij}(\vartheta_i^{\hat{\vartheta}_{i,j-1}}, \vartheta_i^{\hat{\vartheta}_{i,j}}) \leq b_{ij}, \quad (10)$$

where

$$\mathcal{H}_{ij} = e_m(i) e_{n_i}^T(j)$$

and

$$\phi_{ij} \triangleq \phi_{ij}(\vartheta_i^{\hat{\vartheta}_{i,j-1}}, \vartheta_i^{\hat{\vartheta}_{i,j}})$$

for shortness.

Without loss of generality, we assume that  $a_{ij} = 0$  for all  $j = 1, \dots, n_i$  and  $i = 1, \dots, m$ . Indeed, if there exists a subset

$$\mathfrak{B} \triangleq \left\{ (i, j) \in \{1, \dots, m\} \times \{1, \dots, \max(n_i)\} : a_{ij} \neq 0 \right\}$$

such that  $\mathfrak{B} \neq \emptyset$ , then we can rewrite the dynamics equation of the system (6) as

$$\dot{x} = \tilde{A}x + G\tilde{\gamma}(x) + E\omega$$

where

$$\tilde{A} = A + G \sum_{(i,j) \in \mathfrak{B}} a_{ij} \mathcal{H}_{ij} H_i$$

and

$$\tilde{\gamma}(x) = \gamma(x) - \left( \sum_{(i,j) \in \mathfrak{B}} a_{ij} \mathcal{H}_{ij} H_i \right) x.$$

It is quite clear that the new function  $\tilde{\gamma}$  satisfies (10) with  $\tilde{a}_{ij} = 0$  and  $\tilde{b}_{ij} = b_{ij} - a_{ij}$ .

Since  $\vartheta_i - \hat{\vartheta}_i = (H_i - K_i C)e - K_i D\omega$ , then we have

$$\begin{aligned} \gamma(x) - \gamma(\hat{x}) &= \left[ \sum_{i,j=1}^{i,j=m,n_i} \phi_{ij} \mathcal{H}_{ij} (H_i - K_i C) \right] e \\ &\quad - \left[ \sum_{i,j=1}^{i,j=m,n_i} \phi_{ij} \mathcal{H}_{ij} K_i D \right] \omega \quad (11) \end{aligned}$$

The dynamics equation of the estimation error is then given by:

$$\begin{aligned} \dot{e} &= \left( \mathbb{A}_L + \sum_{i,j=1}^{i,j=m,n_i} \left[ \phi_{ij} G \mathcal{H}_{ij} \mathbb{H}_{K_i} \right] \right) e \\ &\quad + \left( \mathbb{E}_L + \sum_{i,j=1}^{i,j=m,n_i} \left[ \phi_{ij} G \mathcal{H}_{ij} \mathbb{D}_{K_i} \right] \right) \omega \quad (12) \end{aligned}$$

with

$$\mathbb{A}_L = A - LC, \quad \mathbb{E}_L = E - LD \quad (13)$$

$$\mathbb{H}_{K_i} = H_i - K_i C, \quad \mathbb{D}_{K_i} = -K_i D \quad (14)$$

The aim consists in finding the gains  $L$  and  $K_i, i = 1, \dots, m$  so that the estimation error dynamics (12) is  $\mathcal{H}_\infty$  asymptotically stable. That is, the objective is to determine the observer parameters such that the following  $\mathcal{H}_\infty$  criterion is satisfied:

$$\|e\|_{\mathcal{L}_2^n} \leq \sqrt{\mu \|\omega\|_{\mathcal{L}_2^q}^2 + \nu \|e_0\|^2} \quad (15)$$

where  $\mu > 0$  is the disturbance attenuation level and  $\nu > 0$  is to be determined. To be more clear,  $\sqrt{\mu}$  is the disturbance gain from  $\omega$  to  $e$ .

As usually for this class of systems concerned by the LMI techniques, we use a quadratic Lyapunov function to analyze the  $\mathcal{H}_\infty$  stability. That is, we use

$$V(e) = e^T \mathbb{P} e, \quad \mathbb{P} = \mathbb{P}^T > 0.$$

Consequently,  $\mathcal{H}_\infty$  criterion (15) is satisfied if the following inequality holds (Zemouche and Boutayeb, 2009):

$$\mathcal{W} \triangleq \dot{V}(e) + \|e\|^2 - \mu \|\omega\|^2 \leq 0. \quad (16)$$

This problem has been handled in the literature and several methods have been proposed where each method provides increasingly relaxed LMI condition (Arcak and Kokoć, 2001), (Chong *et al.*, 2012), (Açikmese and Corless,

2011), (Zemouche and Boutayeb, 2009). It turned out that all these techniques provide conservative LMI conditions. Despite all the new ways to improve the existing techniques, the problem of observer design for Lipschitz nonlinear systems remains a challenge to solve. This is the motivation of the proposed results.. Detailed discussions on the limitations of all these methods compared to the proposed design methodology are presented in Section 4.

## 2.2 Preliminary result

Before presenting an extended version for systems with nonlinear outputs and giving some useful discussions and application to vehicle dynamics, we first recall the main contribution of Zemouche *et al.* (2016) as a preliminary result.

**Theorem 4 (Zemouche *et al.* (2016))** *If there exist symmetric positive definite matrices  $\mathbb{P} \in \mathbb{R}^{n \times n}$ ,  $\mathcal{Z}_i \in \mathbb{R}^{n_i \times n_i}$  and matrices  $\mathcal{R} \in \mathbb{R}^{p \times n}$ ,  $\mathcal{F}_i \in \mathbb{R}^{p \times n_i}$  of appropriate dimensions so that the following convex optimization problem is solvable:*

$$\min(\mu) \text{ subject to (18)} \quad (17)$$

$$\begin{bmatrix} \mathbb{A}(\mathbb{P}, \mathcal{R}) & \mathbb{P}E - \mathcal{R}^T D \\ \begin{matrix} \star & -\mu \mathbb{I}_q \end{matrix} \\ \begin{matrix} \star & -\Lambda Z \end{matrix} \end{bmatrix} \leq 0 \quad (18)$$

with

$$\mathbb{A}(\mathbb{P}, \mathcal{R}) = A^T \mathbb{P} + \mathbb{P}A - C^T \mathcal{R} - \mathcal{R}^T C + \mathbb{I}_n \quad (19)$$

$$\Sigma_i = [\mathcal{N}_1(\mathbb{P}, \mathcal{F}_i, \mathcal{Z}_i) \dots \mathcal{N}_{n_i}(\mathbb{P}, \mathcal{F}_i, \mathcal{Z}_i)] \quad (20)$$

$$\mathcal{N}_j(\mathbb{P}, \mathcal{F}_i, \mathcal{Z}_i) = \begin{bmatrix} \mathbb{P}G\mathcal{H}_{ij} \\ 0 \end{bmatrix} + \begin{bmatrix} H_i^T \mathcal{Z}_i - C^T \mathcal{F}_i \\ -D^T \mathcal{F}_i \end{bmatrix} \quad (21)$$

$$\Lambda = \text{block-diag}(\Lambda_1, \dots, \Lambda_m) \quad (22)$$

$$\Lambda_i = \text{block-diag} \left( \frac{2}{b_{i1}} \mathbb{I}_{n_i}, \dots, \frac{2}{b_{in_i}} \mathbb{I}_{n_i} \right) \quad (23)$$

$$Z = \text{block-diag}(Z_1, \dots, Z_m) \quad (24)$$

$$Z_i = \text{block-diag} \left( \overbrace{\mathcal{Z}_i, \dots, \mathcal{Z}_i}^{n_i \text{ times}} \right) \quad (25)$$

then, the  $\mathcal{H}_\infty$  criterion (15) is satisfied with  $v = \lambda_{\max}(\mathbb{P})$ . Hence, the observer gains  $L$  and  $K_i$  will be computed by

$$L = \mathbb{P}^{-1} \mathcal{R}^T, \quad K_i = \mathcal{Z}_i^{-1} \mathcal{F}_i^T.$$

**PROOF.** See Zemouche *et al.* (2016).

## 3 Systems with Nonlinear Outputs

In the aim to increase application of the proposed design method, we propose in this section an extension to systems with nonlinear outputs. This case is often encountered in many real applications, such as the problem of magnetic position estimation and automotive slip angle estimation problem. We consider the following class of systems:

$$\begin{cases} \dot{x} = Ax + G\gamma(x) + E\omega \\ y = Cx + Bg(x) + D\omega \end{cases} \quad (26)$$

where  $B \in \mathbb{R}^{p \times s}$  is a constant matrix and  $g(\cdot)$  is the nonlinear part of the output signal, which is assumed to be globally Lipschitz. We can write  $g(x)$  under the detailed form:

$$g(x) = \begin{bmatrix} g_1(F_1 x) \\ \vdots \\ \theta_i \\ g_i(F_i x) \\ \vdots \\ g_s(F_s x) \end{bmatrix}$$

with  $F_i \in \mathbb{R}^{p_i \times n}$ . The other matrices and parameters are defined in Section 2.1.

The state observer structure we consider in this case is as follows:

$$\dot{\hat{x}} = A\hat{x} + G \begin{bmatrix} \gamma_1(\hat{\vartheta}_1) \\ \vdots \\ \gamma_i(\hat{\vartheta}_i) \\ \vdots \\ \gamma_m(\hat{\vartheta}_m) \end{bmatrix} + L(y - \hat{y}) \quad (27a)$$

$$\hat{y} = C\hat{x} + B \begin{bmatrix} g_1(\hat{\theta}_1) \\ \vdots \\ g_i(\hat{\theta}_i) \\ \vdots \\ g_s(\hat{\theta}_s) \end{bmatrix} \quad (27b)$$

$$\hat{\vartheta}_i = H_i \hat{x} + K_i (y - \hat{y}) \quad (27c)$$

$$\hat{\theta}_i = F_i \hat{x} + M_i (y - z) \quad (27d)$$

$$z = C\hat{x} + B \begin{bmatrix} g_1(F_1 \hat{x}) \\ \vdots \\ g_i(F_i \hat{x}) \\ \vdots \\ g_s(F_s \hat{x}) \end{bmatrix}. \quad (27e)$$

The matrices  $L \in \mathbb{R}^{n \times p}$ ,  $K_i \in \mathbb{R}^{n_i \times p}$  and  $M_i \in \mathbb{R}^{p_i \times p}$  are to be determined so that the estimation error  $e = x - \hat{x}$  converges asymptotically towards zero.

Since  $g(\cdot)$  is globally Lipschitz, then from Lemma 2 there exist functions

$$\psi_{ij} : \mathbb{R}^{p_i} \times \mathbb{R}^{p_i} \rightarrow \mathbb{R}$$

and constants  $c_{ij}, d_{ij}$ , such that

$$g(x) - g(\hat{x}) = \sum_{i,j=1}^{i,j=q,p_i} \psi_{ij} \mathcal{F}_{ij} (\theta_i - \hat{\theta}_i) \quad (28)$$

$$c_{ij} \leq \psi_{ij} (\vartheta_i^{\hat{\vartheta}_{i,j-1}}, \vartheta_i^{\hat{\vartheta}_{i,j}}) \leq d_{ij}. \quad (29)$$

and without loss of generality, we assume that  $c_{ij} = 0$ .

Since  $\theta_i - \hat{\theta}_i = (F_i - M_i C)e - M_i D\omega$ , then we have

$$g(x) - g(\hat{x}) = \begin{bmatrix} \sum_{i,j=1}^{i,j=q,p_i} \psi_{ij} \mathcal{F}_{ij} (F_i - M_i C) \\ - \sum_{i,j=1}^{i,j=q,p_i} \psi_{ij} \mathcal{F}_{ij} M_i D \end{bmatrix} e \quad (30)$$

Consequently, the dynamics equation of the estimation error is given by:

$$\begin{aligned} \dot{e} = & \left( \mathbb{A}_L + \sum_{i,j=1}^{i,j=m,n_i} \left[ \phi_{ij} G \mathcal{H}_{ij} \mathbb{H}_{K_i} \right] \right) e \\ & + \left[ \sum_{i,j=1}^{i,j=q,p_i} \psi_{ij} L B \mathcal{F}_{ij} \mathbb{F}_{M_i} \right] e \\ & + \left( \mathbb{E}_L + \sum_{i,j=1}^{i,j=m,n_i} \left[ \phi_{ij} G \mathcal{H}_{ij} \mathbb{D}_{K_i} \right] \right) \omega \\ & + \left[ \sum_{i,j=1}^{i,j=q,p_i} \psi_{ij} L B \mathcal{F}_{ij} \mathbb{D}_{M_i} \right] \omega \end{aligned} \quad (31)$$

with

$$\mathbb{F}_{M_i} = -(F_i - M_i C), \quad \mathbb{D}_{M_i} = M_i D \quad (32)$$

Following the proof of Theorem 4 given in Zemouche *et al.* (2016), we deduce that  $\mathcal{W}$  defined in (16) is semi-negative definite if the following inequality is fulfilled:

$$\begin{aligned} & \overbrace{\begin{bmatrix} \mathbb{A}_L^T \mathbb{P} + \mathbb{P} \mathbb{A}_L + \mathbb{I}_n & \mathbb{P} \mathbb{E}_L \\ \mathbb{E}_L^T \mathbb{P} & -\mu \mathbb{I}_q \end{bmatrix}}^{\text{LINEAR}} \\ & + \sum_{i,j=1}^{i,j=m,n_i} \phi_{ij} \left( \begin{bmatrix} \mathbb{X}_{ij}^T \\ \mathbb{P} G \mathcal{H}_{ij} \\ 0 \end{bmatrix} \begin{bmatrix} \mathbb{Y}_i \\ \mathbb{H}_{K_i} & \mathbb{D}_{K_i} \end{bmatrix} + \mathbb{Y}_i^T \mathbb{X}_{ij} \right) \\ & + \sum_{i,j=1}^{i,j=q,p_i} \psi_{ij} \left( \begin{bmatrix} \tilde{\mathbb{X}}_{ij}^T \\ \mathbb{P} L B \mathcal{F}_{ij} \\ 0 \end{bmatrix} \begin{bmatrix} \tilde{\mathbb{Y}}_i \\ \mathbb{F}_{M_i} & \mathbb{D}_{M_i} \end{bmatrix} + \tilde{\mathbb{Y}}_i^T \tilde{\mathbb{X}}_{ij} \right) \leq 0. \end{aligned} \quad (33)$$

From Lemma 3 we get the following inequalities for all symmetric positive definite matrices  $\mathbb{S}_{ij}$  and  $\mathbb{M}_{ij}$ :

$$\mathbb{X}_{ij}^T \mathbb{Y}_i + \mathbb{Y}_i^T \mathbb{X}_{ij} \leq \frac{1}{2} (\mathbb{X}_{ij} + \mathbb{S}_{ij} \mathbb{Y}_i)^T \mathbb{S}_{ij}^{-1} \overbrace{(\mathbb{X}_{ij} + \mathbb{S}_{ij} \mathbb{Y}_i)}^{\Delta_{ij}} \quad (34)$$

$$\tilde{\mathbb{X}}_{ij}^T \tilde{\mathbb{Y}}_i + \tilde{\mathbb{Y}}_i^T \tilde{\mathbb{X}}_{ij} \leq \frac{1}{2} (\tilde{\mathbb{X}}_{ij} + \mathbb{M}_{ij} \tilde{\mathbb{Y}}_i)^T \mathbb{M}_{ij}^{-1} \overbrace{(\tilde{\mathbb{X}}_{ij} + \mathbb{M}_{ij} \tilde{\mathbb{Y}}_i)}^{\tilde{\Delta}_{ij}}. \quad (35)$$

Inspired from (Zemouche *et al.*, 2016, Theorem 1), we obtain the following more general theorem valid for systems with nonlinear outputs.

**Theorem 5** Assume that there exist symmetric positive definite matrices  $\mathbb{P} \in \mathbb{R}^{n \times n}$ ,  $\mathcal{L}_i \in \mathbb{R}^{n_i \times n_i}$ ,  $\mathcal{S}_i \in \mathbb{R}^{p_i \times p_i}$  and matrices  $\mathcal{R} \in \mathbb{R}^{p \times n}$ ,  $\mathcal{F}_i \in \mathbb{R}^{p \times n_i}$ ,  $\tilde{\mathcal{F}}_i \in \mathbb{R}^{p \times p_i}$  of appropriate dimensions so that the following convex optimization problem is solvable:

$$\min(\mu) \text{ subject to (37)} \quad (36)$$

$$\begin{bmatrix} \left[ \begin{array}{c|c} \mathbb{A}(\mathbb{P}, \mathcal{R}) & \mathbb{P}E - \mathcal{R}^T D \\ \hline (*) & -\mu \mathbb{I}_q \end{array} \right] & \overbrace{\begin{bmatrix} \Sigma \\ \Sigma_1 \dots \Sigma_m \end{bmatrix}}^{\Sigma} & \text{OUT}_{13} \\ & & \\ & (*) & -\Lambda Z & 0 \\ & (*) & (*) & \text{OUT}_{33} \end{bmatrix} \leq 0 \quad (37)$$

with

$$\text{OUT}_{13} = \begin{bmatrix} \bar{\Sigma}_1 \dots \bar{\Sigma}_q \end{bmatrix} \quad (38)$$

$$\text{OUT}_{33} = -\Pi S \quad (39)$$

$$\bar{\Sigma}_i = \begin{bmatrix} \bar{\mathcal{N}}_1(\mathcal{R}, \bar{\mathcal{T}}_i, \mathcal{S}_i) \dots \bar{\mathcal{N}}_{p_i}(\mathcal{R}, \bar{\mathcal{T}}_i, \mathcal{S}_i) \end{bmatrix} \quad (40)$$

$$\bar{\mathcal{N}}_j(\mathcal{R}, \bar{\mathcal{T}}_i, \mathcal{S}_i) = \begin{bmatrix} \mathcal{R}^T B \mathcal{F}_{ij} \\ 0 \end{bmatrix} + \begin{bmatrix} -\left( F_i^T \mathcal{S}_i - C^T \bar{\mathcal{T}}_i \right) \\ D^T \bar{\mathcal{T}}_i \end{bmatrix} \quad (41)$$

$$\Pi = \text{block-diag}(\Pi_1, \dots, \Pi_q) \quad (42)$$

$$\Pi_i = \text{block-diag} \left( \frac{2}{d_{i1}} \mathbb{I}_{p_i}, \dots, \frac{2}{d_{ip_i}} \mathbb{I}_{p_i} \right) \quad (43)$$

$$\mathbb{S} = \text{block-diag}(\mathbb{S}_1, \dots, \mathbb{S}_q) \quad (44)$$

$$\mathbb{S}_i = \text{block-diag} \left( \overbrace{\mathcal{S}_i, \dots, \mathcal{S}_i}^{p_i \text{ times}} \right) \quad (45)$$

where the other variables are defined in Theorem 4.

Then, the  $\mathcal{H}_\infty$  criterion (15) is satisfied with  $\nu = \lambda_{\max}(\mathbb{P})$ . Hence, the observer gains  $L$ ,  $K_i$  and  $M_i$  are computed by

$$L = \mathbb{P}^{-1} \mathcal{R}^T, \quad K_i = \mathcal{Z}_i^{-1} \mathcal{T}_i^T, \quad M_i = \mathcal{S}_i^{-1} \bar{\mathcal{T}}_i^T.$$

**PROOF.** The proof is omitted. We can prove Theorem 5 by exploiting inequalities (34)-(35) and using Schur lemma and some change of variables as in the proof of (Zemouche *et al.*, 2016, Theorem 1). The fact that the functions  $\phi_{ij}$  and  $\psi_{ij}$  are bounded and assumed to be positive, without loss of generality, plays an important role in the application of the Young's inequality. Since they are positive, then they are not included in the matrices when the Young's relation is applied in (34)-(35). They are simply replaced by their upper bounds  $b_{ij}$  and  $d_{ij}$ , respectively. For more details, we refer the reader to Zemouche and Boutayeb (2009).

## 4 Constructive Discussions

This subsection is devoted to some comments and remarks to explain the difference between what we proposed and the available methods in the literature related to the same methodology.

### 4.1 On the class of systems

The class of systems concerned by what we proposed in this paper is more general than that in Chong *et al.* (2012). The class of systems is not only defined by inequalities (10) and (29), but it is also distinguished by the matrices  $G, B$  and  $H_i, F_i$ . In case of systems with linear outputs, the matrices  $H_i$  in Chong *et al.* (2012) are particular; they have only one row. Certainly we can generalize the result, but the method used in Chong *et al.* (2012) to introduce a diagonal multiplier matrix as an additional degree of freedom, requires  $H_i$  to be special. However, the method proposed in this paper does not have any restriction on the dependence of the nonlinearities on the state of the system. That is, the matrices  $G$  and  $H_i$  are arbitrary. For a two dimensional system having only one nonlinear component depending on the entire state, the method in Chong *et al.* (2012) fails. For instance, the method in Chong *et al.* (2012) is unable to give solutions for a system with nonlinear component as:

$$\gamma(x) = \begin{bmatrix} 1 \\ 0 \end{bmatrix} \sin(x_1) \cos(x_2).$$

Nevertheless, the method in this paper remains valid and since  $H_1 = \mathbb{I}_2$ , we have a full matrix  $\mathcal{Z}_1 \in \mathbb{R}^{2 \times 2}$  as additional degree of freedom in the LMI (18).

### 4.2 On the diagonal multiplier matrix in Chong *et al.* (2012)

The proposed method is more general than that in Chong *et al.* (2012). Indeed, for  $n_i = 1, \forall i = 1, m$ , we retrieve the diagonal multiplier matrix introduced in Chong *et al.* (2012). It should be noticed that the diagonal multiplier matrix, firstly given in Fan and Arcak (2003) for a special class of structured nonlinearities, is not really an additional degree of freedom. Indeed, this matrix comes from structuring the matrices  $H_i$ , which are not unique. To see clearly the non unicity of  $H_i$ , consider a two dimensional system with a nonlinear term

$$\gamma(x) = \begin{bmatrix} 1 \\ 0 \end{bmatrix} \sin(x_1 + x_2).$$

For the approach in Chong *et al.* (2012), the matrix  $H_1$  should be  $H_1 = [1 \ 1]$ . However, with the proposed method, we have the choice between  $H_1 = [1 \ 1]$  and  $H_1 = \mathbb{I}_2$ . Even better, the latter choice, which is not possible for Chong *et al.* (2012), allows to have more degrees of freedom, namely  $\mathcal{Z}_1 \in \mathbb{R}^{2 \times 2}$ . It is obvious that we can apply the approach in Chong *et al.* (2012) by considering:

$$\gamma(x) = \begin{bmatrix} 1 & 0 \\ 0 & 0 \end{bmatrix} \begin{bmatrix} \sin(x_1 + x_2) \\ 0 \end{bmatrix}$$



with  $H = \begin{bmatrix} 1 & 1 \\ 0 & 1 \end{bmatrix}$ , for example, but this form is useless because the second component of the nonlinearity is null.

In a general way, for systems with scalar nonlinearity, the diagonal multiplier matrix introduced in Chong *et al.* (2012) is useless. Indeed, in this case, their multiplier matrix  $M$  is reduced to a positive scalar  $m_1$ . Hence, if their LMI (Chong *et al.*, 2012, LMI (7)) is feasible for any  $m_1 > 0$ , then it is also feasible for  $m_1 = 1$ . However, with the enhanced design method we proposed, we can always increase the dimension of  $H_1$  to have additional degrees of freedom. For instance,  $\sin(x_1)$  can always be written under the form

$$\sin\left(\overbrace{(x_1 - x_2)}^{\vartheta_1} + \overbrace{x_2}^{\vartheta_2}\right)$$

with

$$H_1 = \begin{bmatrix} 1 & -1 \\ 0 & 1 \end{bmatrix}.$$

It is speculated in Chong *et al.* (2012) that the LMI condition in Zemouche and Boutayeb (2009) is particular and not feasible for the neural mass model presented in Chong *et al.* (2012). It is true that for the same matrices  $H_i$ , the LMI technique in Chong *et al.* (2012) is more general than that in Zemouche and Boutayeb (2009). However, analytically speaking, this statement is not true because of the non uniqueness<sup>2</sup> of the matrices  $H_i$ . Indeed, if the LMI (Chong *et al.*, 2012, LMI (7)) is feasible, then this implies feasibility of LMI (Zemouche and Boutayeb, 2009, LMI (13)) with  $\tilde{H}_i = m_i H_i$  and  $\tilde{b}_i = \frac{1}{m_i} b_i$ . To be more clear, see for instance the function  $\sin(x_1)$  in a two dimensional system. We can always write:

$$\sin(x_1) = \sin\left(\overbrace{[1 \ 0]x}^{\vartheta}\right) = \sin\left(\frac{1}{m_i} \overbrace{[m_1 \ 0]x}^{\tilde{\vartheta}}\right).$$

#### 4.3 On monotonic nonlinearities

The methodology followed in this paper is inspired from Arcak and Kokotovic (2001), Fan and Arcak (2003). Basically,

<sup>2</sup> By considering the same neural mass model in Chong *et al.* (2012), the LMI (Zemouche and Boutayeb, 2009, LMI (13)) is found feasible for

$$H = 10^5 \times \begin{bmatrix} 0 & 0 & 0 & 0 & 0 & 0 & 0.01 & 0 \\ 0 & 0 & 0 & 0 & 2 & 0 & 0 & 0 \\ 1 & -1 & 0 & 0 & 0 & 0 & 0 & 0 \end{bmatrix}$$

with better disturbance attenuation levels.

this methodology was established to deal with systems having non Lipschitz but monotonic nonlinearities. The system is non Lipschitz if there exist  $(i, j)$  such that  $b_{ij} = +\infty$ . In this case, the proposed approach, as well as those in Chong *et al.* (2012), Arcak and Kokotovic (2001), and Fan and Arcak (2003), do not work, unless the disturbances vanish from the output measurements, i.e.:  $D = 0$ . In this case, for the feasibility of (Chong *et al.*, 2012, LMI (7)) and the enhanced LMI (18), it is necessary to have

$$\mathbb{P}G\mathcal{H}_{ij} + H_i^T \mathcal{L}_i - C^T \mathcal{F}_i = 0. \quad (46)$$

For systems with nonlinear outputs, if we have  $b_{ij} = d_{ij} = +\infty$ , then the necessary conditions for the feasibility of (37) are

$$\begin{cases} \mathbb{P}G\mathcal{H}_{ij} + H_i^T \mathcal{L}_i - C^T \mathcal{F}_i = 0, \\ \mathcal{R}^T B \mathcal{F}_{ij} - \left(F_i^T \mathcal{S}_i - C^T \tilde{\mathcal{F}}_i\right) = 0. \end{cases} \quad (47)$$

Nevertheless, the fact that  $\mathcal{L}_i$  and  $\mathcal{S}_i$  are non diagonal may enhance the feasibility of (46) and (47), respectively.

#### 4.4 On the incremental quadratic constraints in Açikmese and Corless (2011)

Before the result by Chong *et al.* (2012), a very nice technique has been introduced in Açikmese and Corless (2011) to deal with the similar problem. Thanks to elegant arguments and the introduction of a new so called *incremental quadratic constraint*, more degrees of freedom have been added to the design. Nevertheless, the unique drawback of this methodology is that these degrees of freedom are to be determined before solving the LMI problem. Indeed, the nonlinearity is assumed to satisfy the incremental quadratic constraint depending on these additional degrees of freedom. What we proposed in this paper is completely different. Thanks to the new variant of Young's inequality, the additional degrees of freedom, namely the matrices  $\mathcal{L}_i$  and  $\mathcal{S}_i$ , are considered as decision variables to be provided by the LMI (37).

Useful parameterizations have been proposed in (Açikmese and Corless, 2011, Section 4.1, Section 5.1) by introducing some matrices as decision variables. However, these matrices are not totally free solutions of the LMI, but only parts of these matrices are returned by the LMI condition. In (Açikmese and Corless, 2011, Section 5.1), for instance, particular parameterizations have been provided for globally Lipschitz and monotonic nonlinearities. It is quite clear from their propositions that our methodology provides more degrees of freedom in the LMI. This is, indeed, due to the use of Lemma 3, which leads to more relaxed LMIs, with larger domain of feasibility. Although the same quadratic Lyapunov function has been used in Fan and Arcak (2003), Açikmese and Corless (2011), Arcak and Kokotovic (2001) and all other references dealing with LMI-based observer design, the use of the proposed new variant of Young's inequality allows additional structure of the decision variables. It is the

strength of this Young's inequality, which is new and original. This is the first time this inequality has been exploited in such a way. One of the advantage of the proposed method compared to that in Aıkmeşe and Corless (2011) is that by our technique it suffices to compute the Lipschitz constants of the partial derivatives of the nonlinearity (if differentiable, else we use Lemma 2) to compute the observer gains from the LMI, instead of searching for a good parameterization of the incremental quadratic inequalities, which can turn out to be complicated in some cases. One of our future work consists in combining the results of Aıkmeşe and Corless (2011) with Lemma 3 in the goal to get more relaxed LMI conditions.

#### 4.5 On the additional number of decision variables

The role of the new variant of Young's relation is interesting in the sense that it allows having more degrees of freedom than the classical use of the inequalities (10) as in Chong *et al.* (2012) and Zemouche and Boutayeb (2009). Indeed, if we proceed as in Chong *et al.* (2012), we get for each  $b_{ij}$  an additional variable  $m_{ij}$ . Then, we obtain a total of

$$n_{\text{add1}} = \sum_{i=1}^{i=m} n_i + \sum_{i=1}^{i=s} p_i$$

additional degrees of freedom. However, with the proposed design technique using the Young's inequality, since the matrices  $\mathcal{L}_i$  and  $\mathcal{S}_i$  are symmetric and non diagonal, we get a total of

$$n_{\text{add2}} = \sum_{i=1}^{i=m} \frac{n_i(n_i + 1)}{2} + \sum_{i=1}^{i=s} \frac{p_i(p_i + 1)}{2}$$

additional degrees of freedom. Hence, with this new methodology, we have

$$n_+ = \sum_{i=1}^{i=m} \frac{n_i(n_i - 1)}{2} + \sum_{i=1}^{i=s} \frac{p_i(p_i - 1)}{2}$$

additional decision variables. In case of systems with linear outputs, we have

$$n_{\text{add1}} = \sum_{i=1}^{i=m} n_i, \quad n_{\text{add2}} = \sum_{i=1}^{i=m} \frac{n_i(n_i + 1)}{2},$$

$$n_+ = \sum_{i=1}^{i=m} \frac{n_i(n_i - 1)}{2}.$$

We have  $n_+ = 0$  if  $n_i = 1, \forall i = 1, \dots, m$ . In such a case, we retrieve the diagonal multiplier matrix as in Chong *et al.* (2012).

In the next section we will show the important role of the non diagonal multiplier matrices through two simple numerical examples.

## 5 Illustrative examples and comparisons

This section is dedicated to simple numerical examples to show the validity and effectiveness of the proposed design methodology. Since we compare the proposed method with the LMI techniques in Chong *et al.* (2012) and Zemouche and Boutayeb (2009), then we consider examples of systems with linear outputs. The nonlinear output case is treated in Section 6 devoted to an application to vehicle slip angle estimation.

### 5.1 Example 1

The aim of this example is to compare the proposed method with those in Chong *et al.* (2012) and Zemouche and Boutayeb (2009). Consider the nonlinear system described by the following parameters :

$$A = \begin{bmatrix} 0 & 1 & 0 \\ 0 & 1 & 1 \\ 0 & 1 & 1 \end{bmatrix}, \quad G = \begin{bmatrix} 1 \\ 0 \\ 0 \end{bmatrix}, \quad C = \begin{bmatrix} 1 & 0 & 1 \end{bmatrix},$$

$$H_1 = \begin{bmatrix} 1 & 0 & 0 \\ 0 & 0 & 1 \end{bmatrix}, \quad E = \begin{bmatrix} 1 \\ 1 \\ 1 \end{bmatrix}, \quad D = 1,$$

and  $\gamma_1 : \mathbb{R}^2 \rightarrow \mathbb{R}$  is a differentiable function, without loss of generality.

#### 5.1.1 Test of feasibility:

Assume that  $\gamma$  satisfies the following condition as in (10):

$$0 < \frac{\partial \gamma}{\partial \vartheta_j}(\vartheta) \leq \theta, \quad j = 1, 2. \quad (48)$$

We will test the feasibility of the LMI (18) for different values of  $\theta$  in the three cases where  $\mathcal{L}_1 = \mathbb{I}_2$  as in Zemouche and Boutayeb (2009),  $\mathcal{L}_1 = \text{diag}(m_1, m_2)$  as in Chong *et al.* (2012), and finally for  $\mathcal{L}_1$  non diagonal symmetric positive definite matrix as in Theorem 4. In each case, we will give the optimal value of  $\sqrt{\mu}$  for each value of  $\theta$ . The results obtained by using LMI toolbox of Matlab are summarized in Table 1. It is quite clear from Table 1 that the proposed design method in Theorem 4 is less conservative and provides solutions when the old ones are unable to work. This shows the effectiveness and significance of the non diagonal matrices  $\mathcal{L}_i$  in LMI (18).

#### 5.1.2 Numerical simulations

For simulations, we take

$$\gamma(\vartheta) = g(\vartheta_1)g(\vartheta_2), \quad g(x) = \frac{1}{1 + e^{-8\theta x}}. \quad (49)$$

Methods	LMI (18) with $\mathcal{Z}_1 = \mathbb{I}_2$ (as in Zemouche and Boutayeb (2009))	LMI (18) with diagonal $\mathcal{Z}_1$ (as in Chong <i>et al.</i> (2012))	LMI (18) with non diagonal $\mathcal{Z}_1$ (Theorem 4)
$\theta = 0.10$	1.5657	1.4923	1.4920
$\theta = 0.25$	2.8831	1.6549	1.6500
$\theta = 0.28$	16.7166	1.6976	1.6898
$\theta = 0.50$	infeasible	2.2708	2.1325
$\theta = 0.70$	infeasible	26.1518	3.1247
$\theta = 0.75$	infeasible	infeasible	3.6340
$\theta = 0.95$	infeasible	infeasible	17.0356

Table 1  
Optimal value of  $\sqrt{\mu}$  for each method: Superiority of Theorem 4

It is easy to show that this function satisfies conditions (48). The numerical simulation is done for two cases,  $\theta = 0.70$  and  $\theta = 0.95$ , respectively. In the second case, a diagonal  $\mathcal{Z}_1$  is unable to provide solutions; the simulation is presented in Figure 1 using a normal gaussian noise variable  $\omega \sim (0, 0.3^2)$  on a finite interval in order to show both performances and asymptotic convergence of the estimation errors. In the case  $\theta = 0.70$ , Figures 2 and 3 show the role of the non diagonal matrix to attenuate the level of the disturbance. The results in Figures 2 and 3 are obtained by using a Monte Carlo simulation. We generated 100 normal gaussian noise variables  $\omega \sim (0, 0.05)$  and then we calculated at each time instant  $t$  the value of the Root Mean Square Error (RMSE). Recall that the RMSE function is defined by

$$\text{RMSE}_t(x) = \sqrt{\frac{1}{100} \sum_{j=1}^{100} \|x(t)\|_j^2}$$

where  $\|x\|_j$  is the  $j^{\text{th}}$  realization of the euclidean norm of the vector  $x(t)$ .

It is clear from Figure 3 that the RMSE is globally better with the proposed LMI design technique using non diagonal multiplier matrices.

In the aim to confirm statistically the theoretical value of  $\sqrt{\mu}$  in the case of  $\theta = 0.70$ , we introduce Figure 4 showing that  $\|e(t)\| - \sqrt{\mu}\|\omega(t)\| \leq 0$ , which leads necessarily to  $\|e\|_{\mathcal{L}_2} \leq \sqrt{\mu}\|\omega\|_{\mathcal{L}_2} \leq 0$  in the interval of simulation. For clarity of the presentation, Figure 4 shows a zoom of the simulation result.

## 5.2 Example 2: Role of non diagonal $\mathcal{Z}_i$ on (46)

Here we introduce a simple case study to show the important role that can play the non diagonal matrices  $\mathcal{Z}_i$  on the equality constraint (46). Let us consider a two dimensional

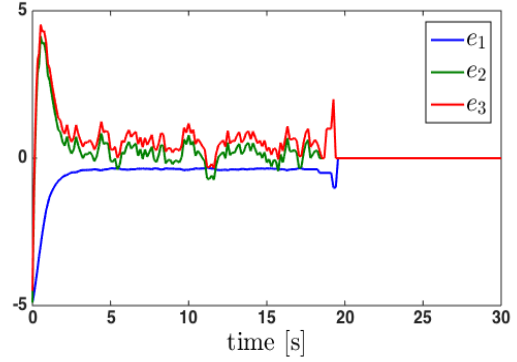


Fig. 1. Estimation errors for  $\theta = 0.95$ .

example of system (6) where the matrices involved in (46) are given as follows:

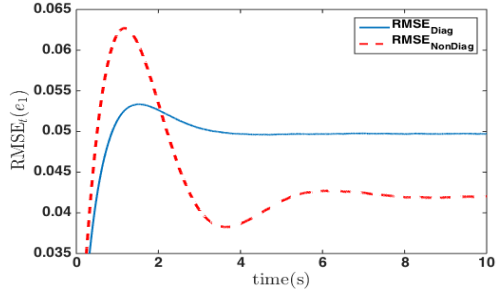
$$G = \begin{bmatrix} 1 \\ 0 \end{bmatrix}, C = \begin{bmatrix} 1 & 1 \end{bmatrix}, H_1 = \begin{bmatrix} 1 & 0 \\ 0 & 1 \end{bmatrix}.$$

This means that we have a single nonlinearity depending on the two state variables  $x_1$  and  $x_2$ . Now, assume that the nonlinearity is not globally Lipschitz with respect to its first argument  $x_1$ . That is,  $b_{11} = +\infty$ . Since  $\mathcal{H}_{11} = \begin{bmatrix} 1 & 0 \\ 0 & 0 \end{bmatrix}$ , then it follows that

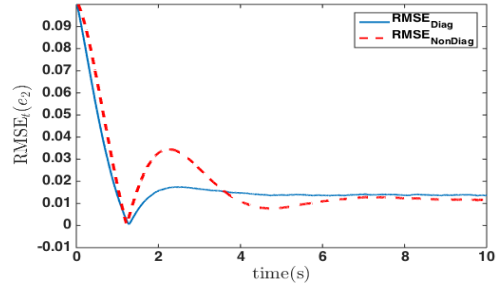
$$\mathbb{P}G\mathcal{H}_{11} = \begin{bmatrix} \mathbb{P}_{11} & 0 \\ \mathbb{P}_{12} & 0 \end{bmatrix}.$$

On the other hand, we have

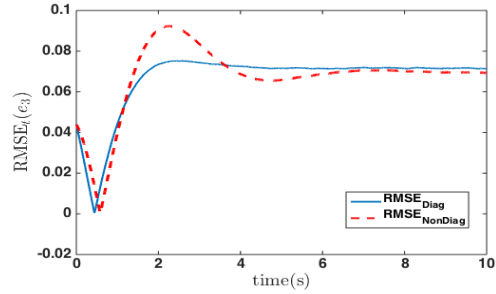
$$H_1^T \mathcal{Z}_1 - C^T \mathcal{T}_1 = \begin{bmatrix} \mathcal{Z}_1^{11} - \mathcal{T}_1^1 & \mathcal{Z}_1^{12} - \mathcal{T}_1^2 \\ \mathcal{Z}_1^{12} - \mathcal{T}_1^1 & \mathcal{Z}_1^{22} - \mathcal{T}_1^2 \end{bmatrix}.$$



(a)  $\text{RMSE}_t(e_1)$ .



(b)  $\text{RMSE}_t(e_2)$ .



(c)  $\text{RMSE}_t(e_3)$ .

Fig. 2.  $\text{RMSE}_t(e_i), i = 1, 2, 3$  with  $\theta = 0.70$ .

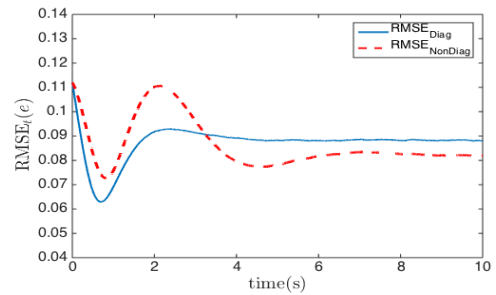


Fig. 3.  $\text{RMSE}_t(e)$  for  $\theta = 0.70$ .

Hence, according to (46), the following equality constraints are necessary:

$$\begin{cases} \mathbb{P}_{11} = \mathcal{T}_1^1 - \mathcal{L}_1^{11} \\ \mathbb{P}_{12} = \mathcal{T}_1^1 - \mathcal{L}_1^{12} \\ \mathcal{L}_1^{12} = \mathcal{T}_1^2 \\ \mathcal{L}_1^{22} = \mathcal{T}_1^2 \end{cases} \quad (50)$$

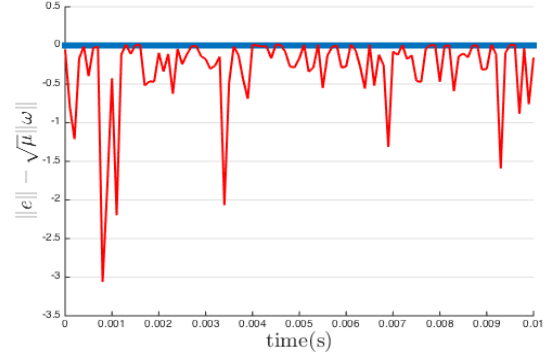


Fig. 4. Zoom on  $\|e\| - \sqrt{\mu}\|\omega\|$  for  $\theta = 0.70$ .

Therefore, if a diagonal matrix  $\mathcal{L}_1$  is used ( $\mathcal{L}_1^{12} = 0$ ) as in Fan and Arcak (2003), Chong *et al.* (2012) and Zemouche and Boutayeb (2009), then we need to have  $\mathcal{T}_1^2 = 0$ , which implies  $\mathcal{L}_1^{22} = 0$ . This contradicts the positive definiteness of  $\mathcal{L}_1$ . We conclude that all the approaches using a diagonal multiplier matrix  $\mathcal{L}_1$  cannot be applied to this example. However, with a non-diagonal  $\mathcal{L}_1$ , the LMI (18) can work provided that (50) holds. Indeed, the equality constraints (50) are not contradictory with the assumptions of Theorem 4. This simple example shows that the non-diagonal matrices  $\mathcal{L}_i$  can enhance the fulfillment of (46) for systems with monotone but not globally Lipschitz nonlinearities.

**Remark 6** *It is worth to point out that the numerical simulations were not the main objective of the two previous simple academic examples (Examples 1 and 2). Indeed, all the solutions provided by the diagonal multiplier based techniques are also solutions for LMI (18) or (37) in the nonlinear output case. Therefore, analytically speaking, it is obvious that the proposed method with non diagonal multiplier matrices is more general because it provides a larger set of solutions, which contains the solutions for diagonal multiplier matrices as a subset. Hence the proposed method is always at least better because the observer gain parameters provided using a diagonal multiplier matrix are particular solutions of the LMI (37) (or (18) in the case of linear outputs).*

## 6 Application to Vehicle Slip Angle Estimation

Electronic stability control (ESC) is a system to prevent vehicles from spinning, drifting out, and rolling over. Several automotive manufacturers have developed and recently commercialized these systems. Most electronic stability control systems focus on yaw rate feedback for enhancing stability performance. However, it would be useful to also control the vehicle slip angle besides controlling yaw rate in situations especially on low-friction road surfaces (Rajamani, 2012). Vehicle slip angle feedback is necessary since too large a value of it can reduce the ability of the tires to generate lateral forces and can endanger the vehicle. Therefore, both yaw rate and vehicle slip angle are variables need for vehicle stability control.

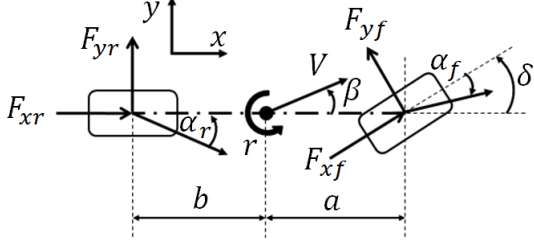


Fig. 5. Single track model for vehicle lateral dynamics

Slip angle cannot be directly measured with reasonably priced sensors on real-world vehicles. Model-based estimation is a suitable method for estimating the vehicle slip angle utilizing only available on-board sensors of the vehicle stability control system. Thus, this section presents a method of estimating the vehicle slip angle based on a nonlinear vehicle model. The developed  $\mathcal{H}_\infty$  observer is validated with experimental measurements on a test vehicle.

### 6.1 Vehicle Lateral Dynamics

The 2 DOF of the vehicle lateral dynamics as shown in Figure 5 consists of the lateral translation of the vehicle and the rotational yaw motion of the vehicle. The nonlinear vehicle lateral dynamics can be formulated as

$$ma_y = (\ddot{y} + ru_x) = F_{yf} + F_{yr} \quad (51)$$

$$I_z \dot{r} = aF_{yf} - bF_{yr} \quad (52)$$

where  $m$  is the mass of the vehicle,  $a_y$  is the lateral acceleration,  $y$  is the lateral translation,  $r$  is the yaw rate,  $u_x$  is the longitudinal velocity,  $F_{yf}$  and  $F_{yr}$  are the lateral tire forces of the front and rear wheels respectively,  $I_z$  is vehicle inertia, and  $a$  and  $b$  are the distances of the front and rear tires respectively from the c.g. of the vehicle.

The lateral tire force for each of the front and rear tires is calculated from a lateral tire model for parabolic normal pressure distribution (Rajamani, 2012):

$$F_y = c_1 \alpha - c_2 \alpha^2 \text{sgn}(\alpha) + c_3 \alpha^3 \quad (53)$$

where  $c_1$ ,  $c_2$ , and  $c_3$  are the coefficient of the tire form model, and  $\alpha$  is the tire slip angle.

The tire slip angle at the front and rear tires can be related to the body slip angle and the yaw rate using the following linear approximations:

$$\alpha_f = \delta - (\beta + ra/u_x), \alpha_r = rb/u_x - \beta \quad (54)$$

where  $\alpha_f$  and  $\alpha_r$  are the tire slip angles of the front and rear wheels respectively,  $\delta$  is the steering angle, and  $\beta$  is the vehicle slip angle.

The vehicle lateral dynamics (51)-(52) including the nonlinear lateral tire model (53) can be rewritten in the standard system dynamics as:

$$\dot{x} = Ax + \bar{B}u + G\gamma(x) + Ew \quad (55)$$

$$y = Cx + Bg(x) + Dw \quad (56)$$

where  $\bar{B} \in R^{(n \times d)}$  is the matrix, and  $u \in R^d$  is the input vector.

This can be done by choosing the front slip angle  $\alpha_f$  and rear slip angle  $\alpha_r$  as the state vector. The system equations can be written as

$$\begin{aligned} \begin{bmatrix} \dot{\alpha}_f \\ \dot{\alpha}_r \end{bmatrix} &= \begin{bmatrix} -\left(\frac{u_x}{a+b} + \frac{a^2 c_{1f}}{I_z u_x}\right) & \left(\frac{u_x}{a+b} + \frac{abc_{1r}}{I_z u_x}\right) \\ -\left(\frac{u_x}{a+b} - \frac{abc_{1f}}{I_z u_x}\right) & \left(\frac{u_x}{a+b} - \frac{b^2 c_{1r}}{I_z u_x}\right) \end{bmatrix} \begin{bmatrix} \alpha_f \\ \alpha_r \end{bmatrix} \\ &+ \begin{bmatrix} \frac{u_x}{a+b} & 1 & -\frac{1}{u_x} \\ \frac{u_x}{a+b} & 0 & -\frac{1}{u_x} \end{bmatrix} \begin{bmatrix} \delta \\ \dot{\delta} \\ \dot{a}_y \end{bmatrix} + \begin{bmatrix} \frac{a^2}{I_z u_x} & -\frac{ab}{I_z u_x} \\ -\frac{ab}{I_z u_x} & \frac{b^2}{I_z u_x} \end{bmatrix} \begin{bmatrix} -\eta(\alpha_f) \\ -\eta(\alpha_r) \end{bmatrix} \\ &+ \begin{bmatrix} 0 \\ 0 \end{bmatrix} w \end{aligned} \quad (57)$$

where  $\eta(\alpha_f) = -c_2 \alpha_f^2 \text{sgn}(\alpha_f) + c_3 \alpha_f^3$ , and  $\eta(\alpha_r) = -c_2 \alpha_r^2 \text{sgn}(\alpha_r) + c_3 \alpha_r^3$ .

The measurement of the system is described by

$$\begin{aligned} \begin{bmatrix} y_1 \\ y_2 \end{bmatrix} &= \begin{bmatrix} r - \left(\frac{u_x}{a+b}\right) \delta \\ a_y \end{bmatrix} = \begin{bmatrix} -\left(\frac{u_x}{a+b}\right) & \left(\frac{u_x}{a+b}\right) \\ \frac{c_{1f}}{m} & \frac{c_{1r}}{m} \end{bmatrix} \begin{bmatrix} \alpha_f \\ \alpha_r \end{bmatrix} \\ &+ \begin{bmatrix} 0 & 0 \\ -\frac{1}{m} & -\frac{1}{m} \end{bmatrix} \begin{bmatrix} -\eta(\alpha_f) \\ -\eta(\alpha_r) \end{bmatrix} + \begin{bmatrix} 0 \\ 0 \end{bmatrix} w \end{aligned} \quad (58)$$

Then, the slip angle of the vehicle can be computed from the slip angle of the front or rear tire as

$$\beta = \delta - \alpha_f - \frac{ra}{u_x} \text{ or } \beta = \frac{rb}{u_x} - \alpha_r. \quad (59)$$

Using the LMI toolbox in Matlab, the observer gain based on Theorem 5 for the model in equations (57)-(59) are found to be



Fig. 6. The Volvo XC90 test vehicle with GPS system (Phanomchoeng *et al.*, 2011)

$$L = \begin{bmatrix} 0.0559 & 0.2677 \\ -0.0471 & 0.3961 \end{bmatrix} \quad (60a)$$

$$K_1 = \begin{bmatrix} -0.0650 & 0.0071 \end{bmatrix}, K_2 = \begin{bmatrix} 0.0650 & 0.0071 \end{bmatrix} \quad (60b)$$

$$M_1 = \begin{bmatrix} -0.0650 & 0.0071 \end{bmatrix}, M_2 = \begin{bmatrix} 0.0650 & 0.0071 \end{bmatrix}. \quad (60c)$$

## 6.2 Experimental Set Up and Results

The test vehicle used for the experimental evaluation is a Volvo XC90 sport utility vehicle. Vehicle testing was conducted at the Eaton Proving Ground in Marshall, Michigan (Piyabongkarn *et al.*, 2009). A MicroAutoBox from dSPACE was used for real-time data acquisition. A real-time 6 axis inertial navigation system combined with GPS, RT3000, from Oxford Technical Solutions was used for these tests to accurately measure the vehicle slip angle for comparison with the performance of the slip angle estimation algorithm. The specification of slip angle estimates from this system according to the manufacturer of the RT3000 is 0.15 degrees. The GPS outputs were connected to the MicroAutoBox via CAN communication at the baud rate of 0.5 Mbits/sec. To obtain objective test results, the vehicle was instrumented to record the relevant values from both CAN network and GPS. The sampling time is set at 2 milliseconds. A photograph of the test vehicle is shown in Figure 6 (Piyabongkarn *et al.*, 2009).

Figures 7 and 8 show the experiment results of a double lane change maneuver with vehicle speed at 70 mph and in a random driving maneuver, respectively. The results shows that the estimated vehicle slip angle can track the vehicle slip angle obtained from the RT3000 system well.

Figure 9 shows the experiment results of double lane change test on a low friction road surface. In this experiment, the friction coefficient of the road surface is changed. However, the same observer gains as (60a)-(60c) are still used for the vehicle slip angle estimation. The estimation result obtained is shown in Figure 9. The estimated slip angle is seen to track well the actual vehicle slip angle in the range of approximately  $-8$  to  $+8$  degrees. The estimation cannot track the actual value well, if it is out of this range because the friction road surface is reduced too much. Overall, this

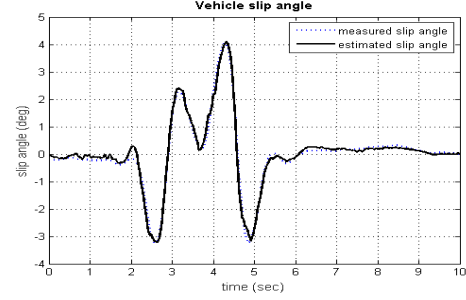


Fig. 7. Vehicle slip angle estimation result in double lane change test.

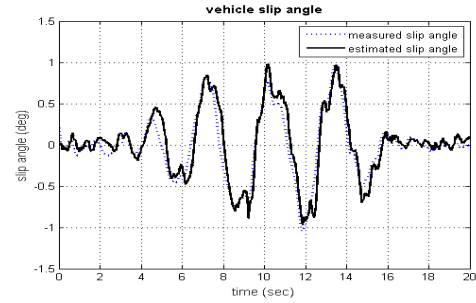


Fig. 8. Vehicle slip angle estimation result in random driving test.

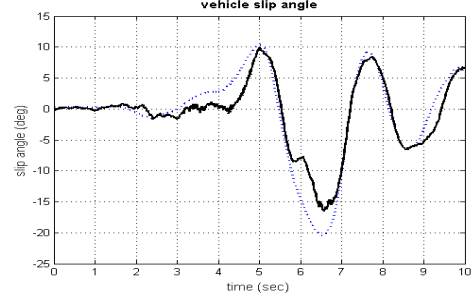


Fig. 9. Vehicle slip angle estimation result in double lane change test on low friction road surface.

observer works successfully even with significant error in assumed friction coefficient value.

If the friction coefficient of the tire-road surface is known, a new observer gain can be obtained. Then, the experiment result of double lane change test on low friction road surface with the new observer gain is shown in Figure 10. It shows that the  $\mathcal{H}_\infty$  observer works very well.

In order to further show the performance of the designed observer, additional disturbances could be applied to the output measurements,  $y$ , and the equation (58) is modified

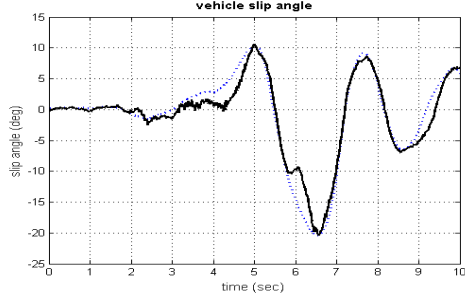


Fig. 10. Vehicle slip angle estimation result in double lane change test on low friction coefficient of the road surface.

as follows:

$$\begin{aligned} \begin{bmatrix} y_1 \\ y_2 \end{bmatrix} &= \begin{bmatrix} r - \left(\frac{u_x}{a+b}\right) \delta \\ a_y \end{bmatrix} = \begin{bmatrix} -\left(\frac{u_x}{a+b}\right) \left(\frac{u_x}{a+b}\right) \\ \frac{c_{lf}}{m} & \frac{c_{lr}}{m} \end{bmatrix} \begin{bmatrix} \alpha_f \\ \alpha_r \end{bmatrix} \\ &+ \begin{bmatrix} 0 & 0 \\ -\frac{1}{m} & -\frac{1}{m} \end{bmatrix} \begin{bmatrix} -\eta(\alpha_f) \\ -\eta(\alpha_r) \end{bmatrix} + \begin{bmatrix} 1 \\ 1 \end{bmatrix} w \end{aligned} \quad (61)$$

Then, the new observer gains and the optimal disturbance attenuation level  $\sqrt{\mu}$  based on equations (57), (61), and (59) are found to be

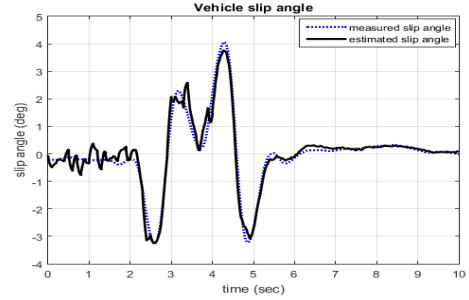
$$L = \begin{bmatrix} -0.1660 & 0.1660 \\ -0.2657 & 0.2657 \end{bmatrix}, \quad \sqrt{\mu} = 1.3359 \times 10^{-2} \quad (62a)$$

$$K_1 = \begin{bmatrix} -0.0059 & 0.0059 \end{bmatrix}, \quad K_2 = \begin{bmatrix} -0.0085 & 0.0085 \end{bmatrix} \quad (62b)$$

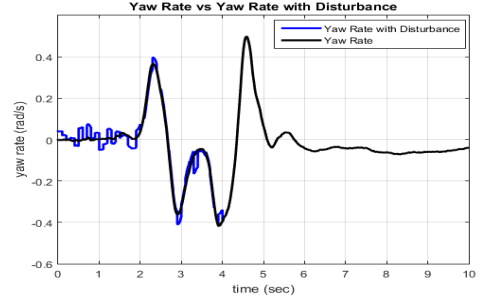
$$M_1 = \begin{bmatrix} -0.0076 & 0.0076 \end{bmatrix}, \quad M_2 = \begin{bmatrix} -0.0119 & 0.0119 \end{bmatrix}. \quad (62c)$$

For the double lane change maneuver with vehicle speed at 70 mph and a random driving maneuver, additional disturbances,  $\omega$ , are added to the lateral acceleration and yaw rate measurements. For the double lane change maneuver, the disturbances for lateral acceleration and yaw rate are Gaussian disturbances with variation of  $0.8m/s^2$ ,  $0.0016rad/s$  respectively. The disturbances are applied during the time 0 to 4 seconds. Likewise, for the random driving maneuver, the disturbances for lateral acceleration and yaw rate are Gaussian disturbances with variation of  $0.4m/s^2$ ,  $0.0008rad/s$  respectively. The disturbances are applied during the time 0 to 8 seconds. The measurements for each case are shown in Figures 11(b)-11(c) and Figures 12(b)-12(c). Then, the vehicle slip angle estimation results are shown in Figures 11(a) and 12(a). The result shows that the estimated vehicle slip angle can track the actual value well even though there are disturbances.

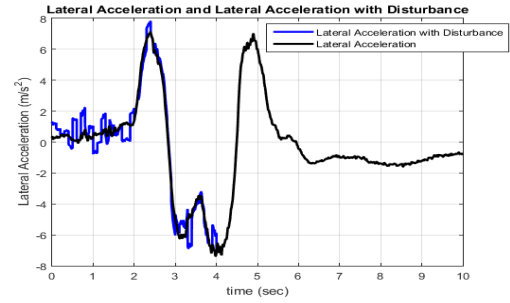
For the double lane change maneuver on a low friction road surface, the disturbances for lateral acceleration and yaw



(a) Vehicle slip angle.



(b) Yaw rate vs yaw rate with disturbance.



(c) Lateral acceleration and lateral acceleration with disturbance.

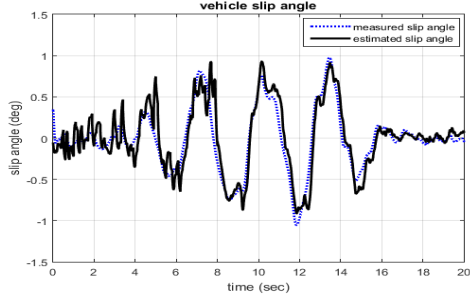
Fig. 11. Results in double lane change test.

rate are Gaussian disturbances with variation of  $0.8m/s^2$ ,  $0.0016rad/s$  respectively. The disturbances are applied during the time 0 to 6 seconds. The measurements are shown in Figures 13(b)-13(c). The observer gains in equations (62) are still used for the vehicle slip angle estimation. Then, the result is shown in Figure 13(a). The estimated slip angle can track well the actual vehicle slip angle only in the range of approximately  $-8$  to  $+8$  degrees since the friction road surface is reduced too much.

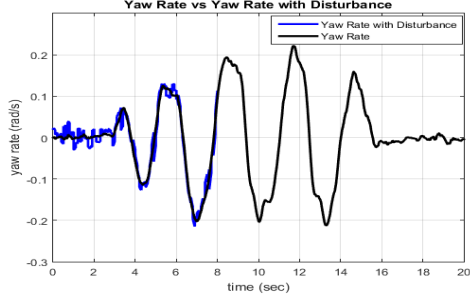
However, if the friction coefficient of the tire-road surface is known, the new observer gain can be re-calculated by Theorem 5. The re-calculated observer gains are shown in equations (63) below.

$$L = \begin{bmatrix} -0.2517 & 0.2517 \\ -1.0096 & 1.0096 \end{bmatrix}, \quad \sqrt{\mu} = 1.3359 \times 10^{-2} \quad (63a)$$

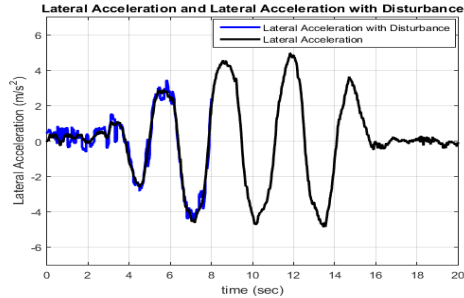




(a) Vehicle slip angle.



(b) Yaw rate vs Yaw rate with disturbance.



(c) Lateral acceleration and lateral acceleration with disturbance.

Fig. 12. Results in random driving test.

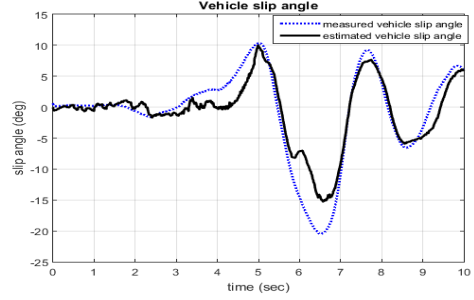
$$K_1 = \begin{bmatrix} -0.0081 & 0.0081 \end{bmatrix}, K_2 = \begin{bmatrix} -0.0091 & 0.0091 \end{bmatrix} \quad (63b)$$

$$M_1 = \begin{bmatrix} -0.0225 & 0.0225 \end{bmatrix}, M_2 = \begin{bmatrix} -0.0336 & 0.0336 \end{bmatrix}. \quad (63c)$$

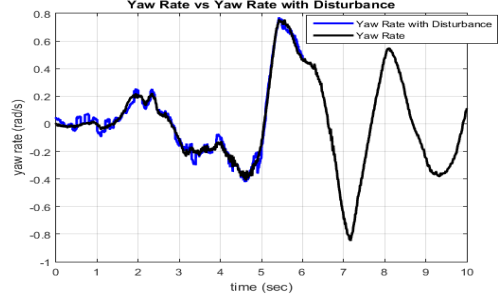
Then, the experiment result of double lane change test on low friction road surface with the re-calculated observer gain is shown on Figure 14. The result shows that the  $\mathcal{H}_\infty$  observer still works very well even with the disturbances.

## 7 Conclusions

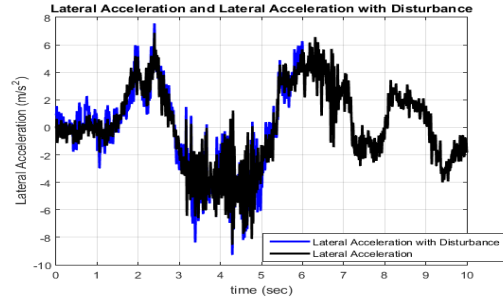
This paper presented a new and less conservative LMI condition to solve the problem of  $\mathcal{H}_\infty$  observer design for a class of Lipschitz nonlinear systems. What we provided in this paper can be seen as a generalization of the work presented in Chong *et al.* (2012) for a more general class of systems. This generalization is done thanks to a new use of the Young's inequality. This novel use of Young's relation has allowed us to introduce a multiplier matrix, which is not



(a) Vehicle slip angle.



(b) Yaw rate vs Yaw rate with disturbance.



(c) Lateral acceleration and lateral acceleration with disturbance.

Fig. 13. Results in double lane change test on low friction road surface.

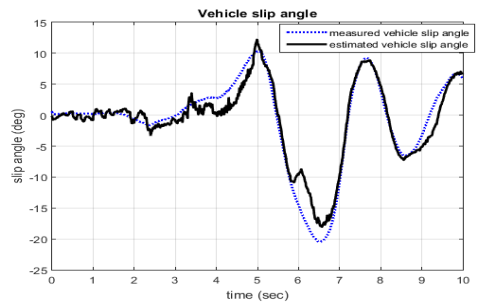


Fig. 14. Vehicle slip angle estimation result in double lane change test on low friction coefficient of the road surface assuming the friction coefficient is known.

necessarily diagonal and enables a less conservative LMI observer design condition. The proposed method is applied experimentally to estimate slip angle for electronic stability control applications in automobiles.



## References

- Abbaszadeh, M. and H. J. Marquez (2010). Nonlinear observer design for one-sided Lipschitz systems. In 'IEEE American Control Conference'. Baltimore, MD, USA.
- Alessandri, A. (2004). 'Design of observers for Lipschitz nonlinear systems using LMI'. *NOLCOS, IFAC Symposium on Nonlinear Control Systems, Stuttgart, Germany*.
- Alessandri, A. and A. Rossi (2013). 'Time-varying increasing-gain observers for nonlinear systems'. *Automatica* **49**(9), 2845–2852.
- Alessandri, A. and A. Rossi (2015). 'Increasing-gain observers for nonlinear systems: Stability and design'. *Automatica* **57**(7), 80–188.
- Andrieu, V., L. Praly and A. Astolfi (2009). 'High gain observers with updated gain and homogeneous correction terms'. *Automatica* **45**(2), 422–428.
- Arcak, M. and P. Kokotovic (2001). 'Observer-based control of systems with slope-restricted nonlinearities'. *IEEE Transactions on Automatic Control* **46**(7), 1146–1150.
- Astolfi, D. and L. Marconi (2015). 'A high-gain nonlinear observer with limited gain power'. *IEEE Transactions on Automatic Control* **60**(11), 3059–3064.
- Astolfi, D., L. Marconi and A. Teel (2016). Low-power peaking-free high-gain observers for nonlinear systems. In 'European Control Conference'. Aalborg, Denmark.
- Açikmese, B. and M. Corless (2011). 'Observers for systems with nonlinearities satisfying incremental quadratic constraints'. *Automatica* **47**(7), 1339–1348.
- Boyd, S., L. El Ghaoui, E. Feron and V. Balakrishnan (1994). *Linear Matrix Inequalities in System and Control Theory*. Vol. 15 of *Studies in Applied Mathematics*. SIAM, Philadelphia, PA.
- Califano, C., S. Monaco and D. Normand-Cyrot (2003). 'On the observer design in discrete-time'. *Systems and Control Letters* **49**, 255–265.
- Chong, M., R. Postoyan, D. Nesić, L. Kuhlmann and A. Varsavsky (2012). 'A robust circle criterion observer with application to neural mass models'. *Automatica* **48**(11), 2986–2989.
- Fan, X. and M. Arcak (2003). 'Observer design for systems with multivariable monotone nonlinearities'. *Systems and Control Letters* **50**, 319–330.
- Gauthier, J. P. and I.A.K. Kupka (1994). 'Observability and observers for nonlinear systems'. *SIAM J. on Control and Optimization* **32**(4), 975–994.
- Gauthier, J. P., H. Hammouri and S. Othman (1992). 'A simple observer for nonlinear systems, applications to bioreactors'. *IEEE Transactions on Automatic Control* **37**(6), 875–880.
- Henriksson, R., M. Norrlöf, S. Moberg, E. Wernholt and T. B. Schön (2009). Experimental comparison of observers for tool position estimation of industrial robots. In 'Proceedings of the 48th IEEE Conference on Decision and Control (CDC) held jointly with 2009 28th Chinese Control Conference'. Shanghai, China.
- Ibrir, S. (2007). 'Circle-criterion approach to discrete-time nonlinear observer design'. *Automatica*.
- Khalil, H. (2002). *Nonlinear Systems*. Prentice Hall, Upper Saddle River, NJ.
- Khalil, H. K. (2015). *Nonlinear Control*. Pearson Education; 1 edition.
- Kravaris, C., V. Sotiropoulos, C. Georgiou, N. Kazantzis, M. Q. Xiao and A. J. Krener (2004). Nonlinear observer design for state and disturbance estimation. In '2004 American Control Conference ACC'04'. Boston, Massachusetts, USA.
- Kravaris, C., V. Sotiropoulos, C. Georgiou, N. Kazantzis, M. Q. Xiao and A. J. Krener (2007). 'Nonlinear observer design for state and disturbance estimation'. *Systems and Control Letters* **56**, 730–735.
- Krener, A. J. and W. Respondek (1985). 'Nonlinear observer with linearizable error dynamics'. *SIAM J. Control and Optimization* **23**(2), 197–216.
- Oueder, M., M. Farza, R. Ben Abdenour and M. M'Saad (2012). 'A high gain observer with updated gain for a class of MIMO non-triangular systems'. *Systems & Control Letters* **61**(2), 298–308.
- Phanomchoeng, G., R. Rajamani and D. Piyabongkarn (2011). 'Nonlinear observer for bounded jacobian systems, with applications to automotive slip angle estimation'. *IEEE Transactions on Automatic Control* **56**(5), 1163–1170.
- Piyabongkarn, D., R. Rajamani, J. Grogg and J. Lew (2009). 'Development and experimental evaluation of a slip angle estimator for vehicle stability control'. *IEEE Transactions on Control Systems Technology* **17**(1), 78–88.
- Raghavan, S. and J. K. Hedrick (1994). 'Observer design for a class of nonlinear systems'. *Int. J. of Control* **59**(2), 515–528.
- Rajamani, R. (2012). *Vehicle Dynamics and Control*. 2nd edition, Springer Verlag.
- Simon, D. (n.d.). *Optimal State Estimation*. John Wiley & Sons, Hoboken, 1st Edition, 2006.
- Thau, F. E. (1973). 'Observing the state of nonlinear dynamic systems'. *International Journal of Control* **17**(3), 471–479.
- Tsinias, J. (2008). 'Time-varying observers for a class of nonlinear systems'. *Systems & Control Letters* **57**(12), 1037–1047.
- Wang, L., D. Astolfi, L. Marconi and H. Su (2017). 'High-gain observers with limited gain power for systems with observability canonical form'. *Automatica* **75**(1), 16–23.
- Zemouche, A. and M. Boutayeb (2009). 'A unified  $\mathcal{H}_\infty$  adaptive observer synthesis method for a class of systems with both Lipschitz and monotone nonlinearities'. *Systems & Control Letters* **58**(4), 282–288.
- Zemouche, A. and M. Boutayeb (2013). 'On LMI conditions to design observers for Lipschitz nonlinear systems'. *Automatica* **49**(2), 585–591.
- Zemouche, A., R. Rajamani, B. Boukroune, H. Rafaralahy and M. Zasadzinski (2016).  $\mathcal{H}_\infty$  circle criterion observer design for Lipschitz nonlinear systems with enhanced LMI conditions. In 'IEEE American Control Conference'. Boston, MA, USA.